

Original Article

The behavioral sensitivity of mice to acetate esters

Liam Jennings¹, Ellie Williams¹, Marta Avlas¹, Adam Dewan^{1*}

Department of Psychology, Florida State University, Tallahassee, FL, United States

*Corresponding author: Department of Psychology, Florida State University, 1107 W. Call St, Tallahassee, FL 32306, United States. Email: dewan@psy.fsu.edu

Abstract

Measures of behavioral sensitivity provide an important guide for choosing the stimulus concentrations used in functional experiments. This information is particularly valuable in the olfactory system as the neural representation of an odorant changes with concentration. This study focuses on acetate esters because they are commonly used to survey neural activity in a variety of olfactory regions, probe the behavioral limits of odor discrimination, and assess odor structure–activity relationships in mice. Despite their frequent use, the relative sensitivity of these odorants in mice is not available. Thus, we assayed the ability of C57BL/6J mice to detect seven different acetates (propyl acetate, butyl acetate, pentyl acetate, hexyl acetate, octyl acetate, isobutyl acetate, and isoamyl acetate) using a head-fixed Go/No-Go operant conditioning assay combined with highly reproducible stimulus delivery. To aid in the accessibility and applicability of our data, we have estimated the vapor-phase concentrations of these odorants in five different solvents using a photoionization detector-based approach. The resulting liquid-/vapor-phase equilibrium equations successfully corrected for behavioral sensitivity differences observed in animals tested with the same odorant in different solvents. We found that mice are most sensitive to isobutyl acetate and least sensitive to propyl acetate. These updated measures of sensitivity will hopefully guide experimenters in choosing appropriate stimulus concentrations for experiments using these odorants.

Key words: olfaction, psychophysics, behavior

Introduction

Perceptual measures of detection threshold provide a mechanism to compare sensory systems across species and gauge appropriate stimulus concentrations for functional experiments. This information is particularly valuable in the olfactory system as odorants are encoded in a combinatorial fashion across glomeruli in the main olfactory bulb (Malnic et al. 1999), with each glomerulus corresponding to a specific receptor (Ressler et al. 1994; Vassar et al. 1994; Mombaerts et al. 1996). These neural representations are not static as the repertoire of activated receptors/glomeruli changes with odorant concentration (Kauer and White 2001), while percepts such as odor identity often (but not always) remain stable (Laing et al. 2003; Mainland et al. 2014). These observations, combined with recent findings, suggest that each receptor/glomerulus does not make an equal contribution to the perception of an odor (Dewan et al. 2013, 2018; Saraiva et al. 2016; Sato-Akudara et al. 2016; Horio et al. 2019; Chong et al. 2020). One potential mechanism to identify receptors/glomeruli that make a significant to the perception of a particular odor, would be to sparsen the representation of the stimulus, by probing the system nearer to its perceptual limits. However, for many odorants, behavioral thresholds have not been identified.

Acetate esters are commonly used to assess odor structure–activity relationships, probe behavioral responses, and survey odor-evoked activity in the brain of mice (Wachowiak and Cohen 2001; Otazu et al. 2015; Kida et al. 2018; Pashkovski et al. 2020; Xu et al. 2020). The stimulus concentrations

used in these studies vary widely as no systematic survey of acetate sensitivity exists in this species. A systematic survey of acetate sensitivity is available for another rodent species, the rat (Moulton 1960). However, the unusual method of stimulus delivery (small nylon capsules attached to a water bottle) would seemingly lessen the applicability of these sensitivity measures for functional studies employing more conventional methods of odor delivery. Behavioral thresholds for specific acetates are available for rats and mice but differ in their behavioral method, the manner of odor delivery, and the solvent used (Moulton 1968; Davis 1973; Pierson 1974; Walker and O’Connell 1986; Slotnick and Schoonover 1993; Clevenger and Restrepo 2006). Thus, depending on the study, sensitivity estimates for these acetates differ by several orders of magnitude. One potential consequence of this variability and lack of a systematic analysis is that functional studies may be employing higher than ideal odorant concentrations.

One major impediment to these cross-study comparisons is an inability to accurately compare vapor-phase odorant concentrations across laboratories. One key factor is a lack of data describing the relationship between the liquid- and vapor-phase concentrations of odorants in different solvents. Raoult’s law for ideal solutions assumes a proportionality between the number of molecules present in the vapor phase and the molar fraction of the solute. In other words, a 10-fold liquid dilution should have 10-fold fewer molecules in the headspace above the liquid. Unfortunately, the vapor-phase concentration of an odorant frequently deviates from these laws of proportionality due to interactions with the solvent

(Haring 1974). Liquid/vapor-phase equilibria measurements are available for several acetate esters diluted in mineral oil (Cometto-Muñiz et al. 2003) but not for other commonly used solvents.

Panels of structurally similar odorants are typically presented at equivalent concentrations to map odor-evoked responses (Uchida et al. 2000; Pashkovski et al. 2020). Large variations in behavioral sensitivity toward these odorants could potentially obfuscate fundamental principles of odor coding. The relationship between sensitivity and acetate carbon chain length can be described as a U-shaped function for several, but not all, of the species tested (Moulton 1960; Laska and Seibt 2002; Hernandez Salazar et al. 2003; Cometto-Muñiz et al. 2008). This relationship has yet to be analyzed in mice.

The goal of the current study was to determine the olfactory detection thresholds of C57BL/6J mice (the most commonly used inbred strain) to acetate esters using operant conditioning combined with a well-controlled and highly reproducible stimulus delivery system. Using a photoionization detector (PID)-based approach, we provide liquid/vapor-phase equilibria equations for these odorants in 5 commonly used solvents. These results will hopefully guide experimenters in choosing appropriate concentrations for functional studies using these odorants and allow more accurate comparisons of acetate concentrations across laboratories.

Methods

Animals

Male and female C57BL/6J mice (25 M; 21 F) were housed in same-sex cages until head-bar surgery. Mice (10–14 weeks old) were anesthetized with isoflurane at a dosage of 2%–3% in oxygen, and administered buprenorphine (0.1 mg/kg) as an analgesic, and lidocaine (2 mg/kg) as a local anesthetic. Mice were secured in a stereotaxic head holder with non-rupture ear bars during the duration of the procedure. A custom titanium head bar (<1 g) and 2–3 micro-screws were affixed to the skull and secured using dental cement. The ID number of the animal was added to the head bar to ensure correct identification throughout the experiment.

After surgery, mice were individually housed and given at least 3 days to recover. Following recovery, mice were water restricted for at least 2 weeks before training in a water-rewarded conditioning paradigm. The daily allotment of water for each mouse was determined according to their body weight. Mice that weighed 85%–100% of their initial bodyweight received 1 mL of water, while mice that weighed 70%–85% of their initial bodyweight received between 1 and 2 mL of water. All procedures conducted were reviewed and approved by the Florida State University Animal Care and Use Committee.

Odor stimuli and solvents

A set of seven acetates was used: propyl acetate (CAS# 109-60-4), butyl acetate (CAS# 123-86-4), pentyl acetate (CAS# 628-63-7), hexyl acetate (CAS# 142-92-7), octyl acetate (CAS# 112-14-1), isobutyl acetate (CAS# 110-19-0), and isoamyl acetate (CAS# 123-92-2). All odorants were of the highest available purity (>98%) and obtained from Millipore-Sigma. Vapor pressure measurements for each odorant were obtained through a US Environmental Protection Agency

database [Estimation Program Interface [Epi] Suite tool; www.epa.gov/oppt/exposure/pubs/episuite.htm]. Air/mucus odorant partition coefficient (β) for each odorant was calculated based on the following equation (Scott et al. 2014):

$$\log\beta = \log\beta_{\text{water}} - (\log P - 1) \times 0.524$$

where β_{water} is the air/water partition coefficient and P is the octanol/water partition coefficient, both of which were also obtained through [Epi] Suite tool (EPA). Odorants were stored under nitrogen and housed in a chemical storage cabinet (Air Science). A set of five solvents was used: nanopure water, mineral oil (CAS# 8042-47-5), diethyl phthalate (CAS# 84-66-2), dipropylene glycol (CAS# 25265-71-8), and propylene glycol (CAS# 57-55-6). Odorants were diluted within an odor-free chemical safety cabinet with the use of filtered pipette tips. For the behavioral experiments, isoamyl acetate was diluted in both nanopure water and mineral oil. All other odorants were only diluted in mineral oil. The maximum odorant concentration tested was 1:100 dilution (or 1% v/v) in mineral oil for all odorants except isobutyl acetate (1:1,000 dilution or 0.1% v/v in mineral oil).

Quantification of the vapor-phase concentration of acetates in different solvents

The relative vapor-phase concentration of an odorant in each solvent was estimated using a PID (Aurora Scientific). Photoionization detection collects and exposes a vapor sample to a high-intensity ultraviolet light that ionizes the chemical molecules, creating a current that is proportional to the vapor-phase concentration of the odorant (Zhou et al. 2018). However, the net charge resulting from the ionization of a specific vapor concentration differs by chemical. Thus, a correction factor (CF) for each odorant needs to be calculated to determine vapor-phase concentration relative to a standard (e.g. isobutylene gas).

To calibrate our PID, 500 ppm of isobutylene gas (Airgas) was directed to the PID using corrosive-resistant, mass flow controllers (MFC, Alicat Scientific), specifically calibrated for isobutylene. To ensure the accuracy of the PID measurements, the flow from the MFCs matched the suction rate of our PID (900 mL/min). Isobutylene gas was presented at multiple concentrations (500, 200, 100, 50, 20, 10 ppm) for each PID gain (1 \times , 5 \times , 10 \times) using flow dilution. The resulting data fit with an equation that described the relationship between isobutylene concentration and PID voltage for each gain.

To calculate the CF for each tested odorant, a sealed bottle containing a small volume of a pure odorant (0.5–10 μ L) was heated beyond its boiling point. The vapor concentration of this odorant in this sealed container can be determined by:

$$\frac{24.4 \left(\frac{\text{L}}{\text{mol}}\right) \times \text{odorant volume } (\mu\text{L}) \times \text{odorant density } \left(\frac{\text{g}}{\text{mol}}\right) \times 10^6}{1,000 \left(\frac{\text{mg}}{\text{g}}\right) \times \text{odorant MW } \left(\frac{\text{g}}{\text{mol}}\right) \times \text{vessel volume (L)}}$$

With the use of three-way valves, an MFC directed the vaporized sample from the temporarily sealed bottle onto the PID. The resulting voltage was converted to an equivalent isobutylene concentration as determined by the calibration method above. The vapor odorant concentration (within the bottle) was divided by the equivalent isobutylene concentration (as determined by the PID voltage) to calculate the CF for that odorant. This method resulted in CFs that were similar to those published online (e.g. <https://sps-support.honeywell.com/s/article/RAE-Correction-factors-for-PID-sensors>)

Table 1. Liquid-/vapor-phase relationships of acetate esters in different solvents.

	Propyl acetate	Butyl acetate	Pentyl acetate	Hexyl acetate	Octyl acetate	Isobutyl acetate	Isoamyl acetate
CAS #	109-60-4	123-86-4	628-63-7	142-92-7	112-14-1	110-19-0	123-92-2
P ^o (mmHg)	35.10	11.90	4.16	1.45	0.22	18.30	5.67
PID SVC (ppm)	49,647	15,150	5,166	1,519	286 ^a	25,878	9,978
PID CF	3.2	2.5	2.2	1.9	3.3 ^a	2.8	1.9
logβ	-2.18	-2.35	-2.48	-2.60	-2.76	-2.14	-2.28
Ideal	max: 100% 496.5x ^{1.00}	max: 100% 151.5x ^{1.00}	max: 100% 51.7x ^{1.00}	max: 100% 15.2x ^{1.00}	max: 100% 2.9x ^{1.00}	max: 100% 258.8x ^{1.00}	max: 100% 99.8x ^{1.00}
Mineral oil	max: 3.5% 5,924x ^{1.00}	max: 3.5% 1,408x ^{0.92}	max: 3.5% 965.1x ^{0.93}	max: 10% 109.7x ^{0.92}	max: 10% 25.1x ^{0.67}	max: 3.5% 3,040x ^{1.00}	max: 3.5% 1,170x ^{0.95}
Water	max: 1% 20,444x ^{0.95}	max: 1% 18,578x ^{0.97}	max: 0.35% 8,497x ^{0.93}	max: 0.1% 10,777x ^{1.01}	n/a	max: 1% 25,480x ^{1.02}	max: 0.35% 25,782x ^{0.97}
Dipropylene glycol	max: 10% 2,688x ^{0.95}	max: 10% 727.5x ^{0.89}	max: 10% 234.6x ^{0.99}	max: 35% 43.31x ^{0.91}	max: 35% 18.8x ^{0.73}	max: 10% 1,351x ^{0.97}	max: 10% 567.3x ^{1.02}
Propylene glycol	max: 3.5% 7,291x ^{0.98}	max: 3.5% 1,460x ^{0.97}	max: 3.5% 815.4x ^{0.94}	max: 10% 163.5x ^{0.91}	max: 10% 51.6x ^{0.63}	max: 3.5% 2,775x ^{1.01}	max: 3.5% 2,154x ^{0.97}
Diethyl phthalate	max: 35% 2,099x ^{0.94}	max: 35% 446.3x ^{0.91}	max: 35% 241.1x ^{1.01}	max: 35% 43.4x ^{0.93}	max: 35% 10.5x ^{0.74}	max: 35% 772.2x ^{1.00}	max: 35% 319.6x ^{0.92}

Vapor pressures (P^o) values were obtained from the [Epi] Suite tool (EPA). The saturated vapor concentration (SVC) and correction factor (CF) for each odorant were determined experimentally using a photoionization detector (PID), while the air/mucus partition coefficient (β) was calculated (see Methods). Liquid-/vapor-phase equilibrium equations obtained from the data in Fig. 1 are in bold where x is the liquid dilution (% v/v) and the answer is the vapor-phase concentration in ppm. Also shown is the max liquid concentration (% v/v) of each odorant that follows the described relationship.

^aOctyl acetate saturated vapor pressure and correction factor are estimated based on the calculated vapor concentration (see Methods).

(Table 1). Furthermore, our measured saturated vapor concentrations closely matched the predicted vapor concentration above a pure odorant as calculated by the following equation:

$$C \text{ (ppm)} = \frac{P_{\text{vap}}}{P_{\text{atm}}} (10^6)$$

where C is the concentration in ppm, P_{vap} is the vapor pressure of the odorant and P_{atm} is the atmospheric pressure in mmHg at 25°C. Of note, the high boiling point of octyl acetate prevented accurate measurements using this method. Thus, the CF for this odorant was estimated by dividing the calculated vapor concentration (based on odor volatility) by the equivalent isobutylene concentration of the equilibrated headspace above a pure odorant (as measured by the PID). This estimation method yielded similar CFs to those calculated with the above method for the remaining acetates.

To measure the liquid-/vapor-phase relationship of acetates in different solvents, we measured the net charge resulting from the ionization of the headspace above the pure and diluted odorant for each solvent using a calibrated PID (Fig. 1A). Due to its low volatility, octyl acetate was the only odorant that was not flow diluted to ensure maximal PID sensitivity. Extensive tests determined that PID responses in our setup are directly proportional to flow dilution levels. Please note that the liquid-/vapor-phase equilibrium equations are corrected for these flow dilutions. Importantly, the total flow from the MFCs always matched the suction rate of the PID (900 mL/min). Two three-way valves switched between a pressure-balanced empty vial and the sample vial (Fig. 1A) 600 msec before delivery to the PID. This time was necessary to ensure the vial was pressurized and the odorant could reach steady state. During stimulus delivery to the PID, a dual-synchronous three-way solenoid valve (final valve) directed the odor sample to the PID and the clean air to exhaust. The duration of the stimulus was 2 s and the average PID response for each trial

was measured between 500 and 1,500 ms after final valve opening. Five measurements were taken from each sample with 30-s inter-trial interval so that the headspace above the odorant could re-equilibrate. To allow for automation, this setup was controlled by a custom Python Script while PID measurements are recorded using a custom-built Arduino-based behavioral controller. The calibrated net charge for each trial was multiplied by the appropriate CF to determine the vapor-phase odorant concentration resulting from associated liquid dilution. These data were plotted and fitted with a power function ($[C]_{\text{vap}} = a[C]_{\text{liq}}^{\beta}$; Prism GraphPad).

Liquid-/vapor-phase equilibrium equations already existed for five of the seven acetates using the solvent mineral oil (Cometto-Muñiz et al. 2003). While our method is not as accurate or sensitive as gas chromatography (GC) (Cometto-Muñiz et al. 2003), this approach resulted in similar vapor-phase concentration estimates. Specifically, a comparison of extrapolated vapor-phase concentration (from 1:100 to 1:10⁻¹⁵ liquid dilutions) resulting from our respective equations yielded maximum differences less than 4-fold. Specifically, the maximum difference between our estimates of vapor-phase concentration for propyl acetate was 0.3-fold, butyl acetate was 2.3-fold, pentyl acetate was 3.6-fold, and hexyl acetate was 2.3-fold. The saturated vapor concentration of octyl acetate measured in the previous study was only 64 ppm (Cometto-Muniz, personal communication) as compared to our calculated 286 ppm (Table 1). Factoring in this difference, the extrapolated vapor-phase concentration resulting from our respective equations differed only by a maximum of 1.6-fold for this odorant.

Stimulus delivery for behavioral approach

Odorants were delivered using a custom, 8-channel, flow-dilution olfactometer (Dewan et al. 2018; Williams and Dewan 2020; Fig. 2A). Disposable 40 mL amber glass vials

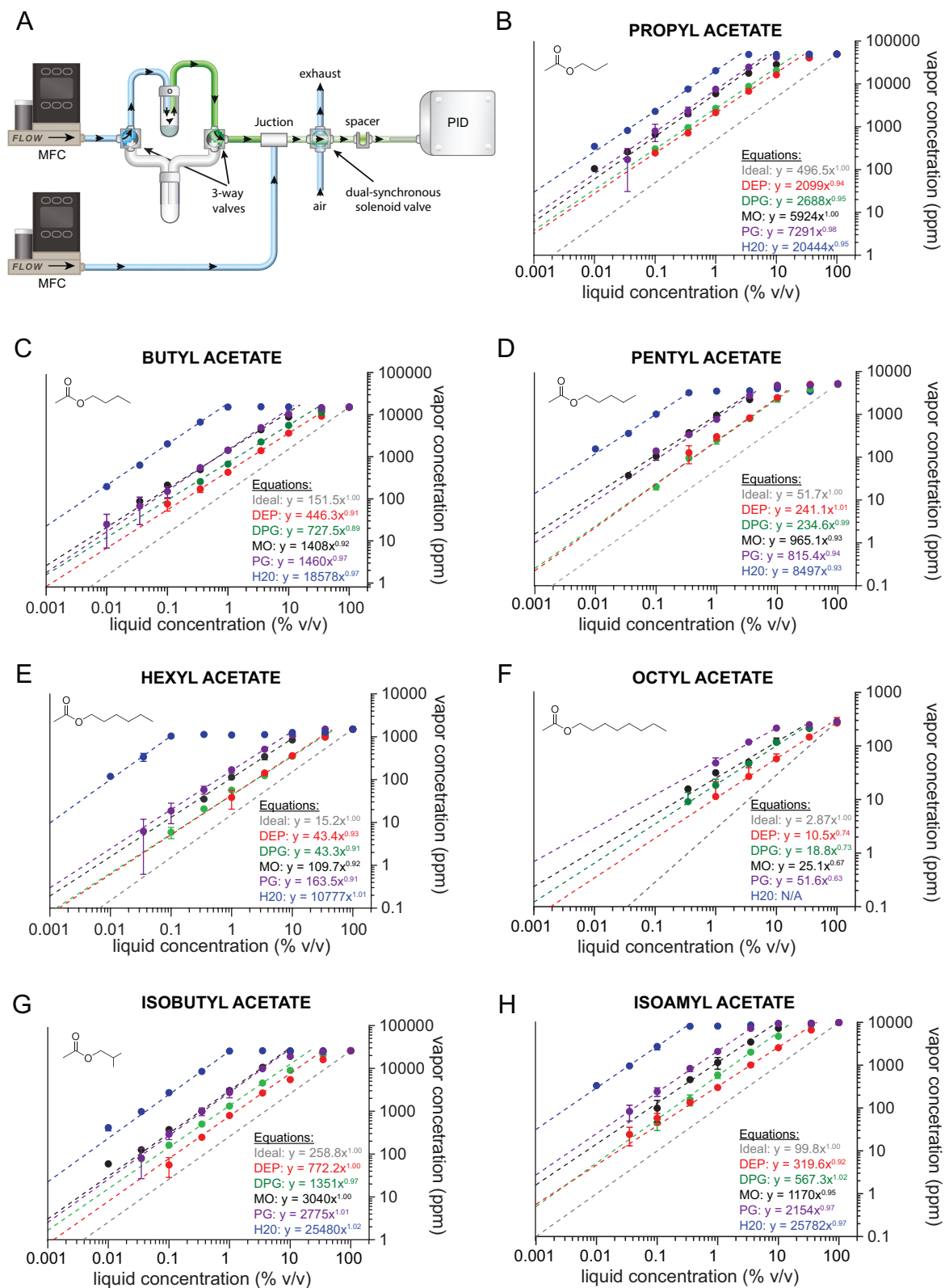


Fig. 1. To approximate the vapor-phase concentration for each odorant/solvent dilution, we used a simplified olfactometer (A). Using mass flow controllers, the diluted headspace above a sample was directed onto a photoionization detector (PID). Two three-way valves switched between a pressure-balanced empty vial (B) and the sample vial (O). A dual-synchronous three-way solenoid valve (final valve) connected the odorized air (~900 mL/min total) and a purified airline (~900 mL/min) to an exhaust line and the odor port. (B–H) Vapor (ppm) versus liquid (% v/v) concentration for seven acetates in logarithmic coordinates. Plots show mean \pm SD for propyl acetate (B), butyl acetate (C), pentyl acetate (D), hexyl acetate (E), octyl acetate (F), isobutyl acetate (G), and isoamyl acetate (H) in five different solvents. The liquid-/vapor-phase equilibrium equation for each solvent ($[C]_{\text{vap}} = a[C]_{\text{liq}}^{\beta}$) is listed in the lower right of each panel, where y denotes the vapor concentration in ppm, x is equal to the liquid concentration (% v/v), and the exponent β is the slope in the double logarithmic coordinates of the figure. See Table 1 for the max concentration for the liquid-/vapor-phase equilibrium equation corresponding to each odorant/solvent pair.

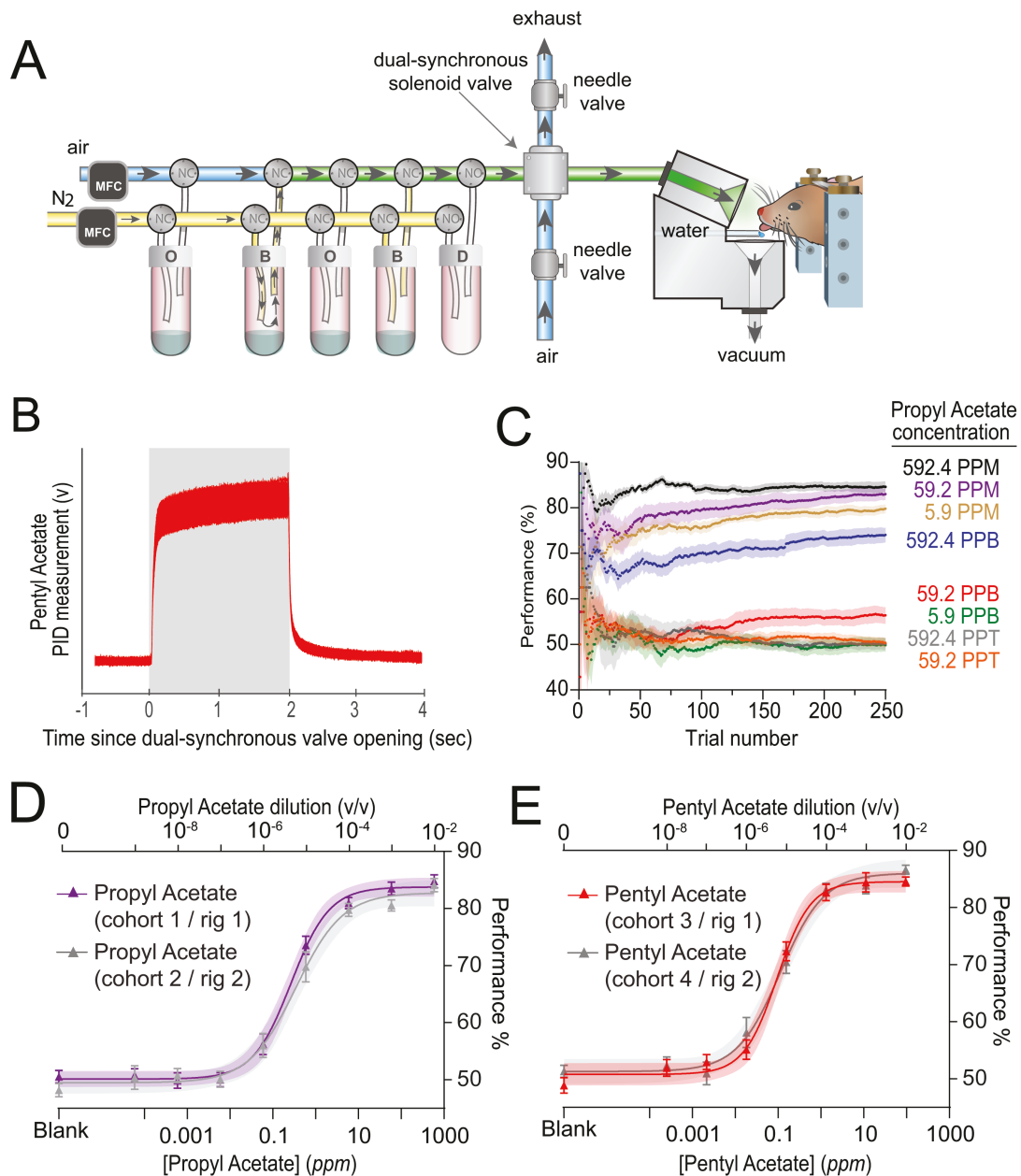


Fig. 2. To measure behavioral detection thresholds, we used a head-fixed Go/No-Go operant conditioning assay combined with well-controlled and highly reproducible stimulus delivery. (A) Odorants were delivered using an 8-channel flow dilution olfactometer that switches between a pressure-balanced dummy (D) vial (via normally open valves, NO) and either odor (O) or blank (B) vials containing only the solvent (via normally closed valves). Odorized air is directed to exhaust to allow the stimulus to reach equilibrium prior to stimulus delivery. During stimulus application, a dual-synchronous solenoid valve re-directs pressure-balanced, odorized air from exhaust to the animal. At the conclusion of the trial, the dual-synchronous solenoid valve returns the pressure-balanced clean air to the animal. (B) Photoionization device (PID) traces of 250 stimulus presentations of propyl acetate. Shaded area signifies 2-s stimulus period. (C) Average cumulative behavioral performance across 250 trials for all concentrations of propyl acetate. Initial go trials are not included. Line signifies mean with shaded SE. Final behavioral performance for each concentration is plotted in the next panel (cohort 2 / rig 2). (D, E) Our experimental approach did not differ across mouse cohorts or different behavioral setups/olfactometers. Data were fitted using a Hill function. Maximal behavioral performance for each odorant concentration is limited to ~85% (see Methods). Plots show mean \pm SE with shaded 95% confidence interval.

filled with 15 mL of diluted odorant (or solvent) were attached to the olfactometer manifolds and pressurized before the start of the first trial. These manifolds switched between a pressure-balanced empty carrier vial (via normally open solenoid valves) and seven odorant vials (via normally closed solenoid valves). Nitrogen gas regulated by a 100 mL/min MFC (Alicat Scientific) flows through the selected vial before it is diluted 10 times by the main air flow stream—regulated

by a 900 mL/min air MFC (Alicat Scientific). Nitrogen was used in the odorized line to minimize the oxidation of the odorant and had no effect on the animal. A dual-synchronous three-way solenoid valve (final valve) connected the olfactometer and a purified airline (~1,000 mL/min) to an exhaust line and the odor port. Care was taken to ensure that both lines were impedance matched to limit pressure spikes during odor delivery. During stimulus delivery, the final valve swapped

the flow to the animal from clean air to diluted odorant. The selected vial within the olfactometer is actuated 0.6-s before stimulus delivery to allow the odor concentration to reach equilibrium before delivery to the animal. The odor port is attached to a micromanipulator to standardize the distance to the nose for each head-fixed animal.

To verify the stability and reproducibility of our odorant presentations, a PID (Aurora Scientific) was used in place of the mouse. A single vial containing 15 mL of the diluted odorant was repeatedly actuated (250 times) with a 15-s inter-trial interval (Fig. 2B, Supplementary Fig. S1). 1% dilution was used for propyl, butyl, pentyl, and isoamyl acetates; a 3.5% dilution was used for isobutyl acetate, and a 10% dilution was used for hexyl and octyl acetates, all using mineral oil as the solvent.

Behavioral assay

Water-restricted mice were trained to report the detection of odor in a Go/No-Go task in a custom-built apparatus, described in detail previously (Dewan et al. 2018; Williams and Dewan 2020; Fig. 2A). Each cohort of mice initially consisted of four males and four females (age-matched). Cohorts were tested on a maximum of two odorants to limit over-training and minimize the probability that mice were solving the task using non-odor cues (see below). Individual mice were excluded from the experiment, if they failed to reach the training criterion ($n = 2$ out of 46) or learned to solve the task using non-odor cues ($n = 1$ out of 46) (see below for specific details).

Behavioral training consisted of two stages. Stage 1—the mice were trained to receive a water reward if they licked during the 2 s stimulus period (signaled by an LED). Stage 2—mice were trained in a Go/No-Go odor detection task. A blank olfactometer vial (15 mL of nanopure water or mineral oil) served as the Go stimulus while a vial containing the highest concentration of the target odor served as the No-Go stimulus (see above for concentrations). Correct responses during the 2 s stimulus period were immediately rewarded with water (1.5–2 μ L) and/or a short inter-trial interval (8–10 s). Incorrect responses were punished with a longer inter-trial interval (13–18 s). Inter-trial intervals were randomized within these ranges to prevent mice from anticipating trial start times. Since over-motivation due to increased thirst can mask true sensitivity (Berditchevskaia et al. 2016), the first 10 trials were Go trials and were not included in our analyses (and are not plotted within the figures). Sessions typically lasted 250–300 trials and were terminated after the mice missed three Go trials in a row or the mice reached 300 trials. Behavioral performance was determined by the number of correct responses (hits + correct rejections) divided by the total number of trials (after the initial Go trials). Mice learned this task quickly and usually performed >90% in the second session. Upon reaching criterion (two sessions >90% correct), mice were subsequently tested in the thresholding assay. Stage 2 training does not include a cheating check (see below), so the maximal behavioral performance is 100% (compared to approximately 85% for the thresholding experiment). Mice that did not reach criterion in a maximum of 4 days were excluded ($n = 2$ out of 46).

To determine behavioral thresholds, mice were only tested on one concentration per day. This approach eliminated any masking/adaptation effects resulting from the contamination

of the olfactometer by higher concentrations of the target odor. The olfactometer was loaded with three blank (Go) vials, three diluted odor (No-Go) vials, and a single blank (No-Go) vial. Each vial was replaced daily, and their positions were randomized. The first session used the same concentration as stage 2 training experiment (see above for concentrations) while each subsequent session presented the mice with a 10-fold dilution of the odorant. Again, mice typically performed 250–300 trials per session and each session was terminated as above. While this approach maximized the length of the session, average behavioral performance stabilized after 100–175 trials (Fig. 2C). The total flow rate (but not flow dilution factor) from the olfactometer was fluctuated (970, 980, 990, or 1,000 mL/min) on a per trial basis to limit mice from using slight variations in air pressure (likely associated with small differences in the resistance of each solenoid/vial combination) to solve the task. The blank No-Go vial (or “cheating check”) served to test whether the mice were using cues other than the presence or absence of the target odor to maximize performance. This blank No-Go vial should be indistinguishable from other blank Go vials unless the animal is using non-odor cues to maximize performance and the associated water reward. Thus, mice are “cheating” at this task if they are able to reject (i.e. not lick) the blank No-Go vial at a frequency higher than the percentage of misses (i.e. not licking during a blank Go vial). If this occurred, the session was excluded from the analysis. If this occurred multiple times over the course of an experiment, the mouse was removed from the experimental group. Since this check is included in our thresholding analysis, the maximum performance a mouse can attain using only odor cues in this experiment is approximately 85% (in contrast to stage 2 training in which the mice can achieve 100% behavioral performance). After the completion of all odorant concentrations, the mouse’s ability to discriminate between vials using non-odor cues was again tested by loading the olfactometer with only blank vials. These data are included in each figure.

Using this setup, the actuation of any single odorant vial resulted in consistent odor kinetics that had <250 ms delay to peak concentration at the mouse’s nose (Williams and Dewan 2020). We have previously shown that mice respond to the stable portion of the odor presentation (not the rapid increase) and that average response times are not correlated with odor concentration (Williams and Dewan 2020).

At the end of each day, the olfactometer (including the manifolds and all tubing) was flushed with acetone, 70% isopropanol, and nanopure water, and then was dried with pressurized clean air overnight. The vial caps and tubing were also cleaned with isopropanol, followed by nanopure water, and dried overnight.

Data analysis

Behavioral performance for each odorant was fitted with a Hill function

$$R = R_{\min} + \frac{R_{\max} - R_{\min}}{\left[1 + \left(\frac{C_{1/2}}{C}\right)^n\right]}$$

where R is the behavioral accuracy, C is odor concentration, $C_{1/2}$ is the concentration at half-maximal performance, and n is the Hill coefficient.

We defined threshold in the standard psychophysical manner as the concentration at which mice discriminate the

odor from blank with 50% accuracy ($C_{1/2}$), typically represented by the inflection point of the psychometric curve (Harvey 1986). Behavioral thresholds were compared between odorants and sexes using a two-way ANOVA with multiple comparisons (Prism GraphPad).

Data availability

The data that support the findings of this study are available from the corresponding author upon reasonable request.

Results

To estimate the vapor-phase concentration of acetates in different solvents, we used a simplified olfactometer and a PID (Fig. 1A). Regardless of the solvent, most acetates showed slopes near unity (i.e. a simple proportionality between the liquid and vapor concentration) at lower concentrations (Fig. 1B–H, Table 1). However, as previously reported (Cometto-Muniz et al. 2003), octyl acetate exhibits a flattening of its slope (Fig. 1F, Table 1). At higher concentrations, all odorant/solvent pairs deviated from this simple proportionality in a solvent-dependent manner (Fig. 1B–H, Table 1). Across the examined concentrations, dilutions in water resulted in the highest vapor concentrations, while dilutions in diethyl phthalate resulted in the vapor concentrations closest to ideal. Interestingly, for most odorants, dilutions in mineral oil and propylene glycol resulted in similar estimations of vapor concentration.

To measure behavioral detection thresholds, we used a head-fixed Go/No-Go operant conditioning assay (Fig. 2A). Our stimulus delivery system resulted in consistent odor pulses throughout a session (Fig. 2B, Supplementary Fig. S1). Although sessions typically lasted 250–300 trials (see Methods for session termination criterion), behavioral performance could be accurately predicted after 150–175 trials (Fig. 2C). As shown previously (Williams and Dewan 2020), our approach is not only consistent among individuals (see below) but even across cohorts of animals. The sensitivity to propyl acetate and pentyl acetate across different cohorts of mice tested in different behavioral

chambers (connected to different olfactometers) were similar (propyl acetate: $P = 0.39$, $F = 0.736$; pentyl acetate: $P = 0.55$, $F = 0.359$, sum of squares test) (Fig. 2D and E). Furthermore, our liquid-/vapor-phase equilibrium equations successfully corrected for behavioral sensitivity differences observed in animals tested with the same odorant in different solvents (Fig. 3).

Mice differed in their sensitivity to these acetates in a manner that was independent of the sex of the animal (odor: $P < 0.0001$, $F(6,43) = 48.82$; sex: $P = 0.407$, $F(1,43) = 0.701$; two-way ANOVA). The average vapor-phase detection threshold for propyl acetate was 268 ppb (95% CI: 189–378 ppb) (Fig. 4A and H). This threshold was equivalent to a 2.1×10^{-6} (95% CI: $1.1\text{--}4.0 \times 10^{-6}$) dilution of propyl acetate in mineral oil (v/v). Individual mice differed in their sensitivity to this odorant by slightly more than one order of magnitude (49–533 ppb).

Mice were not statistically more sensitive to butyl acetate, responding with an average threshold of 49 ppb (95% CI: 35–70 ppb; $P = 0.064$, $df = 43$; two-way ANOVA with multiple comparisons) (Fig. 4B and H). This behavioral threshold was equivalent to a 1.6×10^{-6} (95% CI: $1.1\text{--}2.3 \times 10^{-6}$) dilution of butyl acetate in mineral oil (v/v). Individual mice displayed incredibly consistent thresholds to this odorant, ranging from only 40 to 50 ppb.

The average vapor-phase detection threshold for pentyl acetate was 97 ppb (95% CI: 66–179) (Fig. 4C and H). The animal's sensitivity to this odorant did not differ statistically from propyl acetate ($P = 0.992$) or butyl acetate ($P = 0.271$, $df = 43$, two-way ANOVA with multiple comparisons). This concentration was equivalent to a 7.1×10^{-6} (95% CI: $4.2\text{--}11.8 \times 10^{-6}$) dilution of pentyl acetate in mineral oil (v/v). Individual mice exhibited thresholds that differed by less than one order of magnitude (40–241 ppb).

Mice were more sensitive to hexyl acetate as they had a behavioral threshold of 11 ppb (95% CI: 7–16 ppb) (Fig. 4D and H). Specifically, mice were more sensitive to hexyl acetate than propyl acetate (~24-fold), butyl acetate (~4-fold), and pentyl acetate (~8-fold) ($P < 0.05$, $df = 43$, two-way ANOVA with multiple comparisons; Fig. 4H). The hexyl acetate threshold was equivalent to a 4.4×10^{-6} (95%

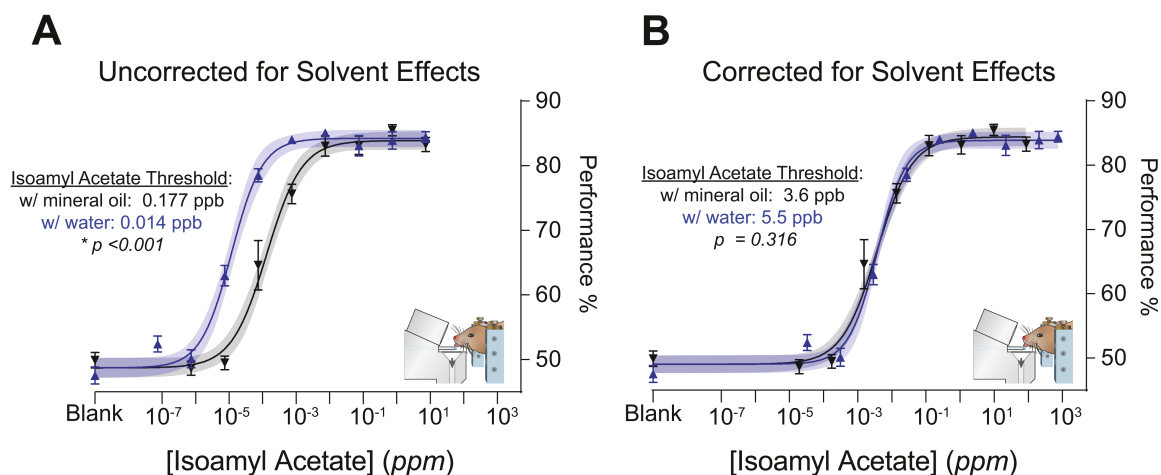


Fig. 3. The resulting liquid-/vapor-phase equilibrium equations successfully corrected for behavioral sensitivity differences observed in animals tested with the same odorant in different solvents. Vapor-phase concentration is plotted according to the ideal (A) or solvent corrected (B) liquid-/vapor-phase equilibrium equation. Data were fitted using a Hill function. Plots show mean \pm SE with shaded 95% confidence interval.

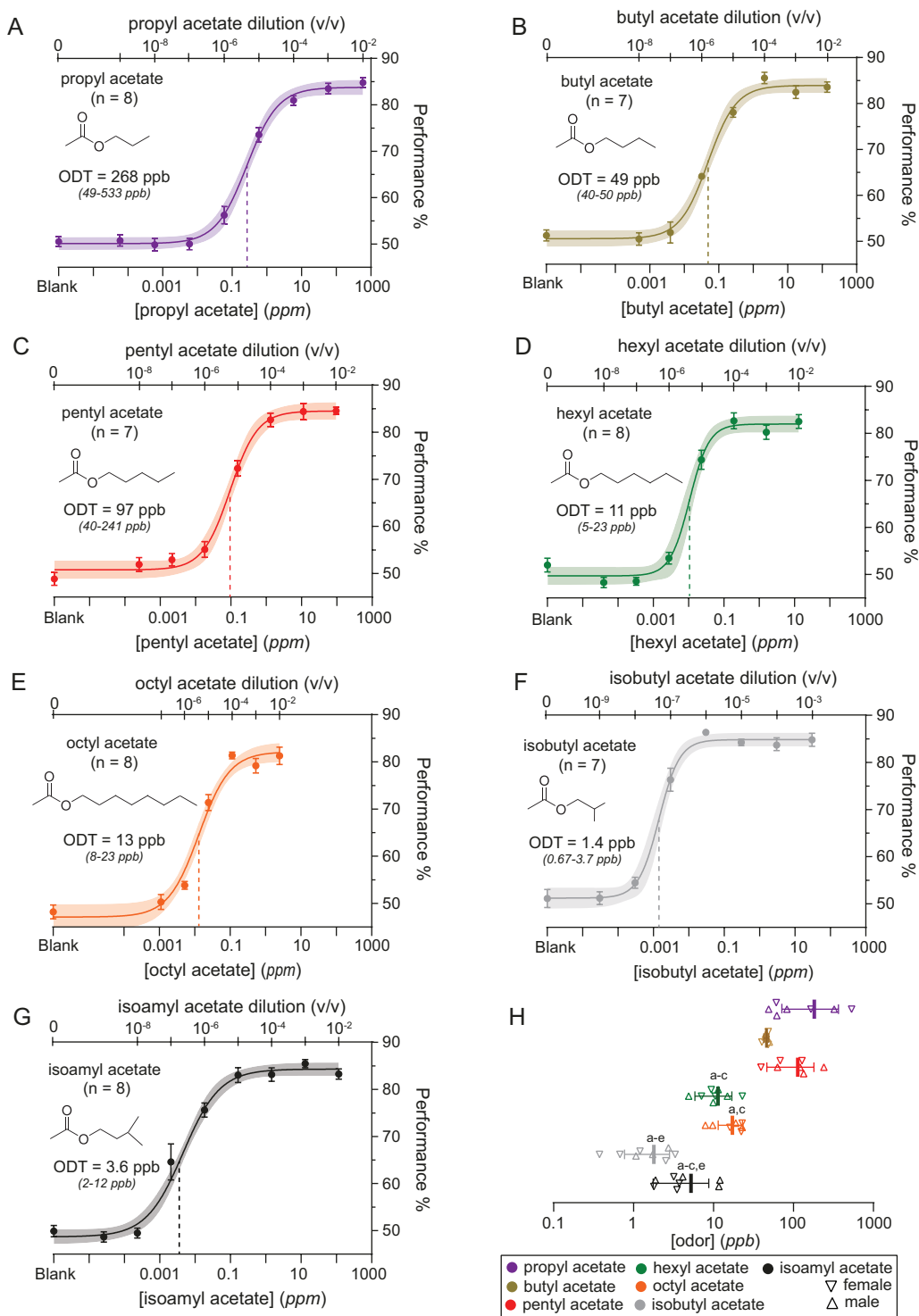


Fig. 4. C57BL/6J mice are sensitive to acetate esters. Psychometric curves to propyl acetate (A), butyl acetate (B), pentyl acetate (C), hexyl acetate (D), octyl acetate (E), isobutyl acetate (F), isoamyl acetate (G), and a summary of all odorants (H). Data were fitted using a Hill function. Maximal behavioral performance for each odor concentration is limited to ~85% (see Methods). Behavioral threshold (ODT) is demarcated with a dashed line (A–G). Plots show mean \pm SE with shaded 95% confidence interval. Top X-axis denotes the liquid dilution tested in the olfactometer. (H) Summary of behavioral sensitivity for all odorants. Plots show mean \pm SD. Individual thresholds for each odorant are denoted with open triangles. Upward triangles denote males while downward triangles denote females. Letters signify statistical differences between two thresholds (a—propyl acetate; b—butyl acetate; c—pentyl acetate; d—hexyl acetate; e—octyl acetate) ($P < 0.05$, two-way ANOVA with multiple comparisons). Statistical significance for these pairwise comparisons is only displayed in one direction.

CI: $2.8\text{--}6.1 \times 10^{-6}$ dilution in mineral oil (v/v). Individual mice differed in their sensitivity to hexyl acetate by less than one order of magnitude (5–23 ppb).

The vapor-phase detection threshold for octyl acetate was 13 ppb (95% CI: 9–19 ppm; Fig. 2E and H). Mice were more sensitive to octyl acetate than either propyl acetate (~20-fold)

or pentyl acetate (~7-fold, $P < 0.001$), but their thresholds were statistically indistinguishable from either butyl acetate or hexyl acetate ($P > 0.05$; $df = 43$, two-way ANOVA with multiple comparisons) (Fig. 4H). The octyl acetate threshold was equivalent to a 4.3×10^{-6} (95% CI: $2.8\text{--}6.5 \times 10^{-6}$) dilution in mineral oil (v/v). Individual mice differed in their sensitivity to octyl acetate by less than one order of magnitude (8–23 ppb).

Mice were most sensitive to isobutyl acetate as they had a behavioral threshold of 1.4 ppb (95% CI: 0.9–1.8 ppb; Fig. 4F and H). Specifically, isobutyl acetate thresholds were lower than those measured for propyl acetate (~190-fold), butyl acetate (~35-fold), pentyl acetate (~70-fold), hexyl acetate (~7-fold), and octyl acetate (~9-fold, $P < 0.05$; $df = 43$, two-way ANOVA with multiple comparisons). The isobutyl acetate threshold is equivalent to a 4.7×10^{-8} (95% CI: $3.25\text{--}6.95 \times 10^{-8}$) dilution of isobutyl acetate in mineral oil (v/v). Individual mice differed in their sensitivity to isobutyl acetate by less than one order of magnitude (0.7–3.7 ppb).

Mice were also very sensitive to isoamyl acetate as they had a behavioral threshold of 3.6 ppb (95% CI: 2.4–5.4 ppb; Fig. 4G and H). Isoamyl acetate thresholds were lower than those of propyl acetate (~80-fold), butyl acetate (~14-fold), pentyl acetate (~27-fold), and octyl acetate (~4-fold, $P < 0.05$; $df = 43$, two-way ANOVA with multiple comparisons). However, the animal's sensitivity to isoamyl acetate was statistically indistinguishable from that of isobutyl acetate and hexyl acetate ($P > 0.05$; $df = 43$, two-way ANOVA with multiple comparisons). The isoamyl acetate threshold was equivalent to a 2.6×10^{-7} (95% CI: $1.7\text{--}4.1 \times 10^{-6}$) dilution in mineral oil (v/v). Individual mice displayed also very similar sensitivities to this odorant (2–12 ppb).

We did not find a statistically significant correlation between olfactory detection thresholds and either carbon chain length ($r_s = -0.752$; $P = 0.142$, Spearman correlation), the volatility of the odorant ($r_s = 0.659$; $P = 0.435$, Spearman correlation), or the air/mucus partition coefficient ($r_s = 0.243$; $P = 0.599$, Spearman correlation) of acetate esters (Table 2).

Discussion

We found that C57BL/6J mice can reliably detect acetate esters at concentrations in the parts per billion (ppb). On average, mice were most sensitive to isobutyl acetate and least sensitive to propyl acetate. Threshold measures did not differ by sex and were relatively consistent across both individuals within a cohort and across different cohorts, even when tested in different behavioral chambers with different olfactometers. These sensitivity data are supplemented by estimations of the vapor concentration of these odorants in different solvents. Although this PID method does not have the sensitivity or accuracy of a GC approach,

it is faster, cheaper, more accessible, and resulted in liquid/vapor-phase equilibrium equations that were very similar to published equations using a purely GC approach (Cometto-Muniz et al. 2003). It is also important to note that our approach is not the first method to use a PID to calibrate odor concentrations (Gorur-Shandilya et al. 2019). In summary, we put forth robust estimates of behavioral sensitivity and vapor concentration that will hopefully guide experimenters in choosing appropriate concentrations for functional studies in mice using these odorants and their preferred solvent.

Estimates of behavioral sensitivity can be influenced by a number of factors, including the behavioral assay, head-fixation, method of odor delivery, strain testing, and the definition of threshold (Bodyak and Slotnick 1999; Slotnick and Schellinck 2002; Tsukatani et al. 2003; Laska 2015). For a detailed discussion about how our method differs from previous studies in these facets, including the addition of a cheating check, please see Williams and Dewan (2020). One additional major impediment to accurately comparing our sensitivity measures to published thresholds is the solvent used. Previous studies have used a wide array of different solvents and in many cases do not account for the odorant/solvent interactions. In fact, our estimates of sensitivity differed by orders of magnitude once the odorant/solvent interactions were factored into our analyses. For example, our uncorrected isoamyl acetate thresholds were overestimated by more than one order of magnitude when diluted in mineral oil and more than two orders of magnitude when diluted in water (Fig. 3). Thus, our uncorrected thresholds differed by an order of magnitude depending on the solvent used. To compare our data more accurately with published studies examining acetate sensitivity, we have provided liquid/vapor-phase equilibrium equations for these odorants in five commonly used solvents.

Our measures of acetate ester sensitivity represent the first behavioral threshold measurements for many of these odorants in mice. Using a maximum likelihood adaptive staircase procedure with dynamic olfactometry, the isoamyl acetate threshold in wild-type mice of the CNGA2 knockout strain was determined to be approximately 32 ppb once the data were corrected for solvent effects (Clevenger and Restrepo 2006). Accordingly, our estimations of isoamyl acetate threshold (2.7 ppb), using the descending method of limits were roughly similar. On the other hand, using a three-stage dynamic flow dilution olfactometer, pentyl acetate thresholds of C57BL/6J mice were approximately 24 parts per trillion (ppt) (Walker and O'Connell 1986), approximately 3 orders of magnitude lower than our estimations of the threshold for this odorant. The reason for this discrepancy is unclear, as our estimations of threshold for this odorant are internally consistent across cohorts of mice and different behavioral chambers (Fig. 2E).

In contrast to the few studies that measured acetate sensitivity in mice, thresholds in rats have been examined multiple

Table 2. Correlation between olfactory detection thresholds and odorant features.

	Carbon chain length	Volatility (mmHg)	Air/mucus partition coefficient (β)
Threshold (ppm)	$r = -0.7523$ $P = 0.142$	$r = 0.6592$ $P = 0.107$	$r = 0.2430$ $P = 0.599$

Spearman's rank correlation coefficients (r_s) are listed along with P value.

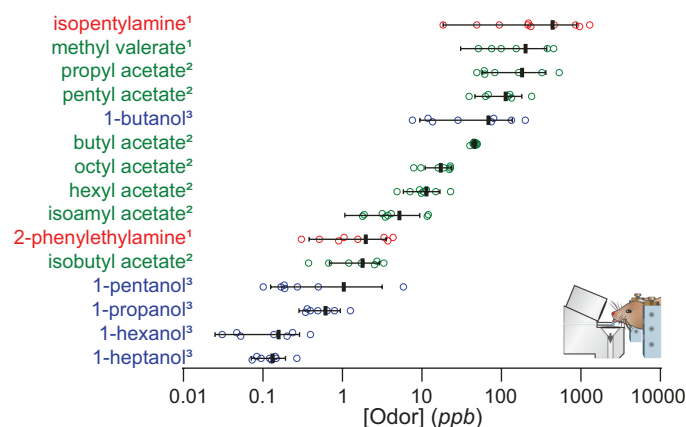


Fig. 5. Summary of olfactory detection thresholds measured with the same approach. Plots show mean \pm SD. Individual thresholds for each odorant are denoted with open circles. Detection thresholds were corrected for solvent effects and obtained from 1—Dewan et al. (2018); 2—current study; 3—Williams and Dewan (2020).

times with varying results. Moulton (1960) measured the sensitivity of rats to several acetates diluted in propylene glycol. Correcting for solvent effects, these thresholds ranged from \sim 50 parts per thousand (ppt) for propyl acetate to \sim 1 ppt for hexyl acetate. Using a different method of odor delivery, the same author updated their estimation of pentyl acetate sensitivity to \sim 4 ppm (corrected) (Moulton 1968). Pierson (1974) and Slotnick and Schoonover (1993) suggested that rats were even more sensitive to these odorants, measuring odor detection thresholds for butyl, pentyl, and hexyl acetates between 1 and 100 ppb. Lastly, Davis (1973) provided the lowest threshold for rats, \sim 5 ppb for pentyl acetate. Clearly, the method of odor delivery and the experimental paradigm can have a profound impact on threshold estimations. However, comparing sensitivity measures within a study indicates that rats are relatively more sensitive to hexyl acetate as compared to propyl acetate, butyl acetate, or pentyl acetate (Moulton 1960; Pierson 1974), similar to our data in mice.

Using the same method, we have previously determined odor detection thresholds for C57BL/6J mice to aliphatic alcohols and wild-type mice of a trace amine-associated receptor knockout strain (129/B6 mixed background) to amines and an additional ester (Dewan et al. 2018; Williams and Dewan 2020). We find that mice are more sensitive to aliphatic alcohols than acetate esters (Fig. 5). Alcohols, carbonyls, and hydrocarbons have been identified as key volatiles produced by grain spoilage fungi (Magan and Evans 2000). Thus, the enhanced sensitivity of mice to alcohols could potentially assist in the identification of spoiled grains, a major food source for both wild and laboratory mice (Pellizzon and Ricci 2020). Interestingly, esters are also targeted by metabolic enzymes secreted in the mouse nasal mucus, resulting in their conversion to the corresponding acids and alcohols (Nagashima and Touhara 2010). Specifically, 20%–40% of aliphatic acetate molecules are converted to the corresponding alcohol, resulting in a significantly lower concentration of the target odorant (Nagashima and Touhara 2010). This mechanism could also contribute to higher behavioral thresholds toward acetates. However, future experiments that measure behavioral thresholds while inhibiting this enzyme-mediated

biotransformation of acetates are necessary to test this hypothesis.

The relationship between acetate sensitivity and the carbon chain length of the odorant appears to differ by species. For rats, acetate sensitivity was found to be negatively correlated with carbon chain length (Moulton 1960), while humans, spider monkeys, squirrel monkeys, and pigtail macaques had a non-linear (i.e. U-shaped) correlation between their olfactory detection thresholds and the carbon chain length of the acetate tested (Laska and Seibt 2002; Hernandez Salazar et al. 2003; Cometto-Muñiz et al. 2008). In mice, acetate sensitivity was not linearly correlated with carbon chain length, odor volatility, or the air/mucus partition coefficient and did not appear to display the U-shaped function observed in other species.

In addition to the main olfactory system, several receptor systems in the nasal cavity can detect airborne chemicals and therefore have the potential to impact detection threshold. In fact, anosmic humans can reliably detect several acetates (methyl to heptyl acetates) (Cometto-Muñiz and Cain 1991). The impact of trigeminal activation on acetate detection has not been investigated in mice. However, olfactory sensitivity to butyl acetate is roughly 6 orders of magnitude lower than trigeminal sensitivity to the same odorant in humans (Cometto-Muñiz et al. 2002). Thus, it seems unlikely that mice are using their trigeminal system to enhance their sensitivity to acetates, but further research is needed.

In summary, we have provided robust estimates of sensitivity in C57BL/6J mice to a series of acetate esters. Interestingly, mice differ in their sensitivity to these odorants, including being more sensitive to the isoform rather than the non-isoform versions of butyl and pentyl acetate. In addition to these threshold measures, we have analyzed the relationship between the liquid- and vapor-phase concentrations of these odorants in five commonly used solvents. It is our hope that these liquid-/vapor-phase equilibrium equations will make our sensitivity measures more accessible and allow more accurate comparisons of vapor-phase acetate concentrations across laboratories.

Supplementary material

Supplementary material is available at *Chemical Senses* online.

Acknowledgments

We thank Fred Fletcher and Te Tang for their help building the operant conditioning rigs as well as coding the Python software; Enrique Cometto-Muniz for advice with odorant/solvent interactions, Chloe Johnson and Sam Caton for early assistance with our photoionization detector-based approach, and Charles Badland for graphic assistance.

Funding

This work was supported by Whitehall Foundation Research Grant [grant number: 2020-05-02].

Conflict of Interest

The authors have no conflict of interest.

References

- Berditchevskaia A, Cazé RD, Schultz SR. Performance in a GO/NOGO perceptual task reflects a balance between impulsive and instrumental components of behaviour. *Sci Rep*. 2016;6:27389.
- Bodyak N, Slotnick B. Performance of mice in an automated olfactometer: odor detection, discrimination and odor memory. *Chem Senses*. 1999;24(6):637–645.
- Chong E, Moroni M, Wilson C, Shoham S, Panzeri S, Rinberg D. Manipulating synthetic optogenetic odors reveals the coding logic of olfactory perception. *Science*. 2020;368(6497):eaba2357.
- Clevenger AC, Restrepo D. Evaluation of the validity of a maximum likelihood adaptive staircase procedure for measurement of olfactory detection threshold in mice. *Chem Senses*. 2006;31(1):9–26.
- Cometto-Muñiz JE, Cain WS. Nasal pungency, odor, and eye irritation thresholds for homologous acetates. *Pharmacol Biochem Behav*. 1991;39(4):983–989.
- Cometto-Muñiz JE, Cain WS, Abraham MH. Quantification of chemical vapors in chemosensory research. *Chem Senses*. 2003;28(6):467–477.
- Cometto-Muñiz JE, Cain WS, Abraham MH, Gil-Lostes J. Concentration-detection functions for the odor of homologous n-acetate esters. *Physiol Behav*. 2008;95(5):658–667.
- Cometto-Muñiz JE, Cain WS, Abraham MH, Gola JMR. Psychometric functions for the olfactory and trigeminal detectability of butyl acetate and toluene. *J Appl Toxicol*. 2002;22(1):25–30.
- Davis RG. Olfactory psychophysical parameters in man, rat, dog, and pigeon. *J Comp Physiol Psychol*. 1973;85(2):221–232.
- Dewan A, Cichy A, Zhang J, Miguel K, Feinstein P, Rinberg D, Bozza T. Single olfactory receptors set odor detection thresholds. *Nat Commun*. 2018;9(1):2887.
- Dewan A, Pacifico R, Zhan R, Rinberg D, Bozza T. Non-redundant coding of aversive odours in the main olfactory pathway. *Nature*. 2013;497(7450):486–489.
- Gorur-Shandilya S, Martelli C, Demir M, Emonet T. Controlling and measuring dynamic odorant stimuli in the laboratory. *J Exp Biol*. 2019;222(23):jeb207787.
- Haring H. Vapor pressures and Raoult's law deviations in relation to odor enhancement and suppression. In: Turk A, Johnston JW, Moulton DG, editors. *Human responses to environmental odors*. New York (NY): Academic Press; 1974. p. 199–226.
- Harvey L. Efficient estimation of sensory thresholds. *Behav Res Methods Instrum Comput*. 1986;18:623–632.
- Hernandez Salazar LT, Laska M, Rodriguez Luna E. Olfactory sensitivity for aliphatic esters in spider monkeys (*Ateles geoffroyi*). *Behav Neurosci*. 2003;117(6):1142–1149.
- Horio N, Murata K, Yoshikawa K, Yoshihara Y, Touhara K. Contribution of individual olfactory receptors to odor-induced attractive or aversive behavior in mice. *Nat Commun*. 2019;10(1):209.
- Kauer JS, White J. Imaging and coding in the olfactory system. *Annu Rev Neurosci*. 2001;24:963–979.
- Kida H, Fukutani Y, Mainland JD, March CA, de Vihani A, Li YR, Chi Q, Toyama A, Liu L, Kameda M, et al. Vapor detection and discrimination with a panel of odorant receptors. *Nat Commun*. 2018;9(1):4556.
- Laing DG, Legha PK, Jinks AL, Hutchinson I. Relationship between molecular structure, concentration and odor qualities of oxygenated aliphatic molecules. *Chem Senses*. 2003;28(1):57–69.
- Laska M. Olfactory discrimination learning in an outbred and an inbred strain of mice. *Chem Senses*. 2015;40(7):489–496.
- Laska M, Seibt A. Olfactory sensitivity for aliphatic esters in squirrel monkeys and pigtail macaques. *Behav Brain Res*. 2002;134(1–2):165–174.
- Magan N, Evans P. Volatiles as an indicator of fungal activity and differentiation between species, and the potential use of electronic nose technology for early detection of grain spoilage. *J Stored Prod Res*. 2000;36(4):319–340.
- Mainland JD, Lundström JN, Reisert J, Lowe G. From molecule to mind: an integrative perspective on odor intensity. *Trends Neurosci*. 2014;37(8):443–454.
- Malnic B, Hirono J, Sato T, Buck LB. Combinatorial receptor codes for odors. *Cell*. 1999;96(5):713–723.
- Mombaerts P, Wang F, Dulac C, Chao SK, Nemes A, Mendelsohn M, Edmondson J, Axel R. Visualizing an olfactory sensory map. *Cell*. 1996;87(4):675–686.
- Moulton DG. Studies in olfactory acuity: III. Relative detectability of n-aliphatic acetates by the rat. *Quart J Exp Psychol*. 1960;12(4):203–213.
- Moulton DG. Electrophysiological and behavioral responses to odor stimulation and their correlation. *Olfactologia*. 1968;1:69–75.
- Nagashima A, Touhara K. Enzymatic conversion of odorants in nasal mucus affects olfactory glomerular activation patterns and odor perception. *J Neurosci*. 2010;30(48):16391–16398.
- Otazu GH, Chae H, Davis MB, Albeanu DF. Cortical feedback decorrelates olfactory bulb output in awake mice. *Neuron*. 2015;86(6):1461–1477.
- Pashkovski SL, Iurilli G, Brann D, Chicharro D, Drumme K, Franks KM, Panzeri S, Datta SR. Structure and flexibility in cortical representations of odour space. *Nature*. 2020;583(7815):253–258.
- Pellizzon MA, Ricci MR. Choice of laboratory rodent diet may confound data interpretation and reproducibility. *Curr Dev Nutr*. 2020;4(4):nzaa031.
- Pierson SC. Conditioned suppression to odorous stimuli in the rat. *J Comp Physiol Psychol*. 1974;86(4):708–717.
- Ressler KJ, Sullivan SL, Buck LB. Information coding in the olfactory system: evidence for a stereotyped and highly organized epitope map in the olfactory bulb. *Cell*. 1994;79(7):1245–1255.
- Saraiva LR, Kondoh K, Ye X, Yoon K-H, Hernandez M, Buck LB. Combinatorial effects of odorants on mouse behavior. *Proc Natl Acad Sci USA*. 2016;113(23):E3300–E3306.
- Sato-Akubara N, Horio N, Kato-Namba A, Yoshikawa K, Niimura Y, Ihara S, Shirasu M, Touhara K. Ligand specificity and evolution of mammalian musk odor receptors: effect of single receptor deletion on odor detection. *J Neurosci*. 2016;36(16):4482–4491.
- Scott JW, Sherrill L, Jiang J, Zhao K. Tuning to odor solubility and sorption pattern in olfactory epithelial responses. *J Neurosci*. 2014;34(6):2025–2036.
- Slotnick B, Schellinck H. Methods in olfactory research with rodents. In: Simon SA, Nicolelis MAL, editors. *Frontiers and methods in chemosenses*. Boca Raton (FL): CRC Press; 2002. p. 21–61.
- Slotnick BM, Schoonover FW. Olfactory sensitivity of rats with transection of the lateral olfactory tract. *Brain Res*. 1993;616(1–2):132–137.
- Tsukatani T, Miwa T, Furukawa M, Costanzo RM. Detection thresholds for phenyl ethyl alcohol using serial dilutions in different solvents. *Chem Senses*. 2003;28(1):25–32.
- Uchida N, Takahashi YK, Tanifuji M, Mori K. Odor maps in the mammalian olfactory bulb: domain organization and odorant structural features. *Nat Neurosci*. 2000;3(10):1035–1043.
- Vassar R, Chao SK, Sitcheran R, Nuñez JM, Vosshall LB, Axel R. Topographic organization of sensory projections to the olfactory bulb. *Cell*. 1994;79(6):981–991.
- Wachowiak M, Cohen LB. Representation of odorants by receptor neuron input to the mouse olfactory bulb. *Neuron*. 2001;32(4):723–735.
- Walker J, O'Connell R. Computerized odor psychophysical testing in mice. *Chem Senses*. 1986;11(4):439–453.
- Williams E, Dewan A. Olfactory detection thresholds for primary aliphatic alcohols in mice. *Chem Senses*. 2020;45(7):513–521.
- Xu L, Li W, Voleti V, Zou D-J, Hillman EMC, Firestein S. Widespread receptor-driven modulation in peripheral olfactory coding. *Science*. 2020;368(6487):eaaz5390.
- Zhou Q, Zhang S, Zhang X, Ma X, Zhou W. Development of a novel micro photoionization detector for rapid volatile organic compounds measurement. *Appl Bionics Biomech*. 2018;2018:5651315.